npj | Materials Degradation

www.nature.com/npjmatdeg

ARTICLE OPEN

Chemical durability of peraluminous glasses for nuclear waste conditioning

Victor Piovesan[1,2,3], Isabelle Bardez-Giboire[1], Maxime Fournier[1], Pierre Frugier[1], Patrick Jollivet[1], Valérie Montouillout[2], Nadia Pellerin[2] and Stéphane Gin[1]

For the handling of high level nuclear waste (HLW), new glass formulations with a high waste capacity and an enhanced thermal stability, chemical durability, and processability are under consideration. This study focuses on the durability of peraluminous glasses in the SiO_2–Al_2O_3–B_2O_3–Na_2O–CaO–La_2O_3 system, defined by an excess of Al^{3+} ions compared with the network-modifying cations Na^+ and Ca^{2+}. To qualify the behavior of such a peraluminous glass in a geological storage situation, its chemical durability was studied in various environments (pure water, groundwater, and alkaline solutions related to a cement environment) and glass alteration regimes (initial rate, residual rate, and resumption of alteration). The alteration solution was characterized by inductively coupled plasma, and the altered glass by scanning electron microscopy, X-ray diffraction and secondary ion mass spectrometry. A comparative study of the chemical durability of these and reference glasses (ISG and SON68) over all timescales highlights the remarkable properties of the former. While their initial dissolution rate is of the same order as the reference glasses, the gel formed under silica saturation conditions is more passivating, making its dissolution rate at least one order of magnitude lower, while its low alkalinity makes it less susceptible to clayey groundwater and highly alkaline solutions.

npj Materials Degradation (2018)2:7 ; doi:10.1038/s41529-018-0028-3

INTRODUCTION

In France, high level nuclear waste is currently immobilized in R7T7 borosilicate glass. The standard procedure for the management of these waste packages over geological time scales is to store them in a deep, low permeability and stable geological formation, such as the Callovo-Oxfordian (COx) claystone that France could choose. R7T7 glass can hold up to 18.5 wt.% of fission products and minor actinides (FPA) and is currently the optimal formulation in terms of thermal stability and long-term behavior.[1–3] However, to improve nuclear reactors efficiency, spent fuel burn-up levels may still continue to increase in the future, leading to higher concentrations of fission products and especially minor actinides in reprocessed spent fuel. To limit the number of vitrified canisters produced, new glass matrices with a higher waste capacity are under study.[4] Glasses with high rare earth (RE) contents are particularly interesting since REs form a substantial proportion of the waste and are commonly used as non-radioactive surrogates for actinides.[5–7]

Two composition ranges, both in the SiO_2–B_2O_3–Al_2O_3–Na_2O–CaO–RE_2O_3 system, have already been explored.[8–16] These two domains of composition are defined by the molar oxides R_P ratio, $R_P = ([M'O] + [M_2O])/([M'O] + [M_2O] + [Al_2O_3])$ with M and M' corresponding to alkaline and alkaline-earth elements, respectively. In a *peralkaline* glass ($R_P > 0.5$), the modifier ions are in excess with respect to the aluminum ions whereas in a *peraluminous* glass ($R_P < 0.5$), the aluminum ions are in excess. The glass network and the structural role of the REs differ substantially in these two composition ranges. In the peralkaline domain, AlO_4 groups are entirely compensated by alkaline and/or alkaline-earth ions, whereas in the peraluminous domain, the AlO_4 groups are compensated by alkaline and alkaline-earth ions but also by RE ions. The alkaline and alkaline-earth elements thus act both as charge compensators and as network modifiers in the peralkaline domain, but principally as charge compensators in the peraluminous domain. The solubility of lanthanides, substantially higher in peraluminous glasses, and their tendency to crystallize, also appear to be strongly dependent on the R_P ratio.[8–11] The potential (i.e., the homogeneity and thermal stability) of peraluminous glasses as HLW conditioning matrices has already been highlighted in a previous study.[15] A candidate composition for long-term studies in contact with aqueous solutions was selected by optimizing its composition as a function of its physico-chemical properties (viscosity, glass transition temperature, density, homogeneity).[16]

The resistance of glass to aqueous alteration is not an intrinsic property of the material, but is rather the response of glass to a range of environmental factors.[17–20] In a closed system, glass dissolution kinetics in contact with water begins by a release of alkaline elements, a process that is rapidly limited by the diffusion rate through the dealkalized glass layer.[21–25] At the same time, the hydrolysis of the glass network leads to the congruent release of the network-forming and -modifying elements. This *initial dissolution period* (or Stage I), continues as long as there is no feedback effect of dissolved elements on the glass dissolution rate. In a given solution (pH, ionic strength) at a fixed temperature, the initial alteration rate (r_0) is the fastest.[26–28] During the *rate drop*, an amorphous layer (or gel) forms that passivate the glass, hindering transport of aqueous species[24,25] and reducing the chemical affinity between the glass surface and the solution.[29–31] Both

[1]CEA, DEN, DE2D SEVT, Bagnols sur Cèze F-30207, France; [2]CNRS CEMHTI-UPR3079, Univ. Orléans, Orléans F-45071, France and [3]AREVA NC/BUR/DT/DRDP, 1 place Jean Millier, Paris La Défense 92084, France
Correspondence: Maxime Fournier (maxime.fournier@cea.fr)

Received: 20 October 2017 Revised: 3 January 2018 Accepted: 5 January 2018
Published online: 02 March 2018

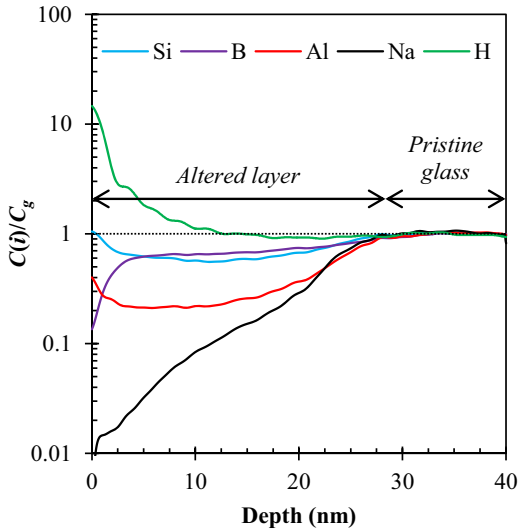

Fig. 1 Elemental profiles measured by ToF-SIMS in G0.40Nd4C glass after dissolution in pure water at 90 °C for two months. Si, B, Al, and Na profiles are normalized with respect to pristine glass (a ratio $C(i)/C_g < 1$ in the altered glass indicates that the altered glass was depleted in element *i* compared to the pristine glass, where $C(i) = (i/\mathrm{Zr})_{\text{altered glass}}$ and $C_g = (i/\mathrm{Zr})_{\text{pristine glass}}$). H profile, due to water and hydroxyl groups in the altered layer, is not normalized

effects lead to a drop in the dissolution rate down to the *residual rate* (Stage II), governed by the precipitation of secondary phases and the reactive transport of hydrated species through the gel.[26,32] Stage III then describes sudden *resumptions of alteration*[33] that can occur, usually for specific glass compositions (e.g., with high alkali metal concentrations) or triggered under specific experimental conditions (e.g., $T \geq 90$ °C and/or pH ≥ 10.5).

Mechanisms and their associated dissolution rates during Stages II and III are mostly governed by the secondary phases that precipitate as the glass degrades, which in turn depend on the composition of the glass and environmental conditions—in particular the composition of the surrounding solution, its renewal rate and the presence of iron and iron corrosion products in the vicinity of the glass.[34–39] For example, the presence of magnesium-containing water (known as COx water) in host rock of the French geological repository is known to lead to the formation of magnesium silicates.[40] Resumption of alteration is also known to be associated with the precipitation of zeolites in alkaline environments.[33,41–45] Since these last minerals contain aluminum, the sensitivity of peraluminous compositions to this phenomenon needs to be investigated.

To acquire an overall understanding of the long-term behavior of peraluminous glasses, the alteration of a peraluminous reference glass, called G0.40Nd4C, was studied in pure and COx water, and in alkaline solutions. The results obtained are compared herein with those in the literature for peralkaline glasses, in particular ISG, the reference standard for the long-term behavior of nuclear glasses,[46,47] and SON68, the radiologically inactive surrogate of the French R7T7 reference nuclear glass.

RESULTS

Choice of alteration tracers

In most studies on borosilicate glass durability, boron is selected as the glass alteration tracer as it is highly soluble and not incorporated in the alteration products. After a leaching period of two months of the G0.40Nd4C glass in pure water at 90 °C and $S/V = 200\ \mathrm{cm}^{-1}$, it is noted that silicon, aluminum, and boron are retained in the altered glass layer (Fig. 1). For silicon and aluminum, this retention is similar to what is observed in peralkaline glasses in which these two elements are involved in the formation of the gel.[26] Boron retention is approximately 30%, as reported previously by Molières et al.[48] for borosilicate glasses rich in lanthanum oxide (SiO_2, B_2O_3, Na_2O, CaO, La_2O_3) and for ISG altered under silica saturation conditions: the boron being retained as undissolved clusters.[49]

Consequently:

- For experiments in pure water, sodium can be used as an alteration tracer for G0.40Nd4C glass because this element is not retained in the altered layer. The alteration rates calculated from boron release rates, underestimated by roughly 30%, are given in comparison with those calculated from the sodium data.
- For experiments performed in COx water or in alkaline solutions, sodium is involved in the formation of secondary phases and thus cannot be used as a dissolution tracer. For these experiments, the (probably underestimated) dissolution rates calculated from boron release rates are given with the caveat that this element is partially retained in the altered layer.

Alteration in pure water

Initial dissolution rate in pure water. Figure 2 shows the equivalent alteration thicknesses measured as a function of time for G0.40Nd4C glass at 100 °C in a Soxhlet device (see also Supplementary Table 1). The initial dissolution rates calculated for Si, Al, B, and Na are 0.8, 0.8, 0.8 and 0.8 $\mathrm{g\,m^{-2}\,d^{-1}}$, respectively, each with an estimated uncertainty of ±0.2 $\mathrm{g\,m^{-2}\,d^{-1}}$.[50]

Residual dissolution rate in pure water. Figure 3 shows the time evolution of the equivalent alteration thicknesses of Si, Al, B, and Na for a static alteration test of G0.40Nd4C glass in pure water at 90 °C and $S/V = 200\ \mathrm{cm}^{-1}$. During the initial stages ($t = 0$ to 56 days), the equivalent thicknesses increase sharply before plateauing. The dissolution rate then decreases slowly.

The dissolution rates calculated between the 210th and 1394th day for Na and B are 2.8×10^{-5} and 2.4×10^{-5} $\mathrm{g\,m^{-2}\,d^{-1}}$, respectively (Supplementary Methods, Supplementary Figure 1 and Supplementary Table 2). The data recorded at $t = 912$ days

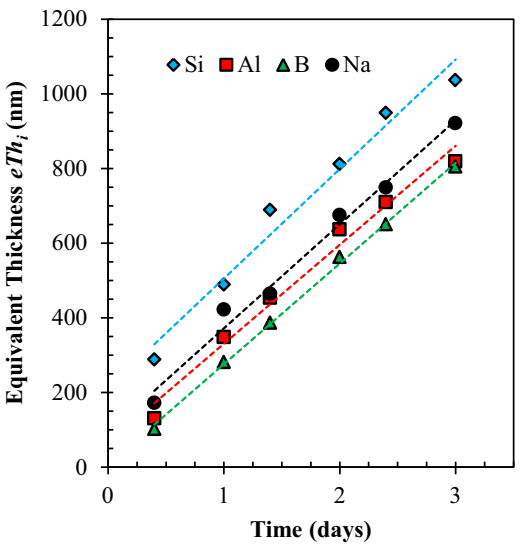

Fig. 2 Initial dissolution rates in pure water. Equivalent alteration thicknesses of Si, Al, B, and Na in G0.40Nd4C glass as a function of time, at 100 °C. The R^2 correlation coefficients for Si, Al, B, and Na are 0.97, 0.99, 1.00, and 0.98, respectively. The pH was ~6.5–7

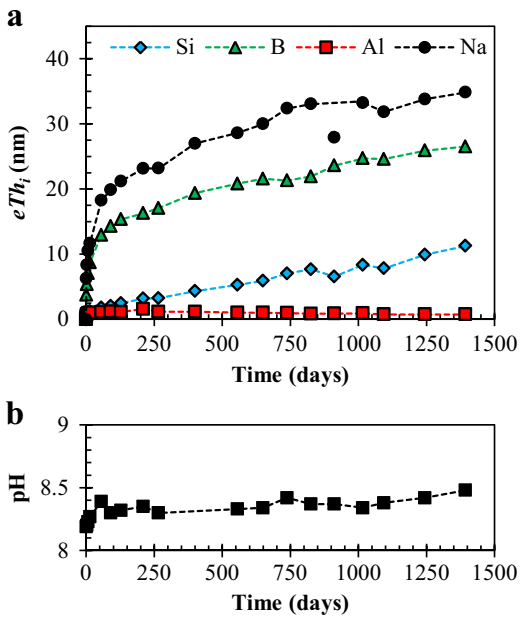

Fig. 3 Residual rates in pure water. **a** Evolution as a function of time of the equivalent alteration thicknesses of Si, B, Al, and Na in G0.40Nd4C glass under static conditions ($T = 90$ °C and $S/V = 200$ cm^{-1}). **b** Time evolution of the pH measured at 90 °C

were not considered in these calculations because of an outlier in the sodium data. The pH over this period was stable at around 8.5 (Fig. 3b).

Alteration in COx water

Figure 4 shows the time evolution of the equivalent alteration thickness of boron, and the magnesium and silicon concentrations, as well as the variation of the pH of the solution during peraluminous G0.40Nd4C glass alteration in COx water at 90 °C and $S/V = 3$ cm^{-1}. The magnesium and silicon concentrations both decrease, the former significantly (Supplementary Table 3). This decrease in the magnesium concentration is accompanied by an order-of-magnitude decrease in the alteration rate, from 3×10^{-3} g m^{-2} d^{-1} between 308 and 486 days to $\approx 5 \times 10^{-4}$ g m^{-2} d^{-1} between 590 and 876 days. The pH of the solution increases during the first few days of leaching before stabilizing after 28 days at about 7.7.

Post-mortem analyses of the solid by X-ray diffraction (XRD) and scanning electron microscopy (SEM) reveal the presence of secondary phases, namely magnesium silicate, neodymium hydroxycarbonate, and calcium sulfate and carbonate (Fig. 5).

Alteration in alkaline environments

Figure 6 shows the time evolutions of the percentage of altered glass calculated from the boron release (an imperfect alteration tracer, cf. section "Choice of alteration tracers"), of the concentrations of aluminum and silicon, and of the pH of the solution during alteration experiments of G0.40Nd4C glass in sodic solutions at 90 °C and $S/V = 40$ cm^{-1}. Note that the pH was regulated for the experiments performed at pH 9.5, 10.5, and 11.3, whereas it was left to vary freely for the experiment initiated at pH 11.5.

For the experiment performed at pH 9.5 (Supplementary Table 4), the percentage of altered glass varies little over time, remaining significantly below 1%.

In the solutions with a pH equal to or greater than 10.5, the altered glass fraction evolves as follows (Fig. 6 and Supplementary Table 5 to Supplementary Table 7):

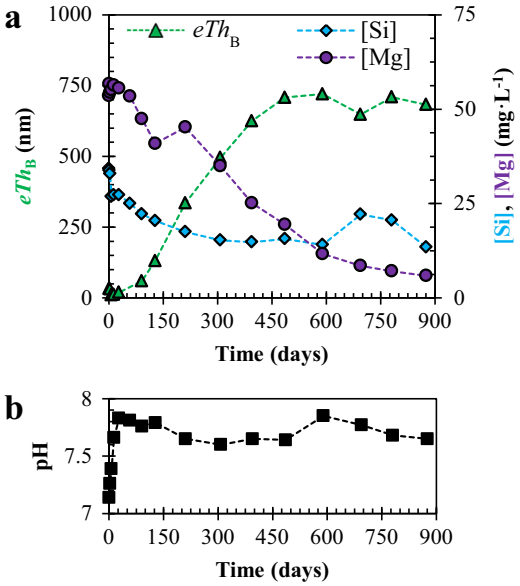

Fig. 4 Alteration in COx water. **a** Time evolution of the equivalent alteration thickness calculated for boron and of the concentrations of magnesium and silicon under static conditions ($T = 90$ °C and $S/V = 3$ cm^{-1}). **b** Evolution of the pH measured at 90 °C

- During an initial "plateau" time period, the altered glass fraction remains low and almost constant (the behavior observed at pH 9.5). The duration of this time period decreases as the pH increases.
- Resumption of alteration: the percentage of altered glass then increases sharply, while the concentrations of aluminum and silicon in solution decrease significantly.
- In the final time period, discussed at greater length in the section "Alteration in pH-controlled solutions", the altered glass fraction stabilizes at a high level, greater than 70%.

Furthermore, in the experiment in which the pH was left to evolve from a starting value of 11.5, the pH decreases as the glass becomes altered (Fig. 6). Alteration then proceeds at a constant rate despite the drop in pH from 11.5 to 9.9, before stopping suddenly.

Post-mortem analyses of the solid by XRD and SEM reveal the presence of zeolites (Fig. 7). For the experiments performed at pH 10.5 and 11.5, Na-P1 type zeolites (body-centered tetragonal lattice) form with the theoretical formula $Na_6Al_6Si_{10}O_{32}{\cdot}12(H_2O)$, whereas for the experiments conducted at pH 11.3, the crystalline phase more closely resembles the orthorhombic Na-P2 zeolite structure, whose theoretical formula is $Na_4Al_4Si_{12}O_{32}{\cdot}14(H_2O)$, or is intermediate between Na-P1 and Na-P2 zeolite structures. In addition, the SEM images of the altered glass show that these zeolites precipitate on the surface of the glass grains. Note that for the glass altered at an initial pH of 11.5, SEM/EDX analyses show that the zeolites formed have Si/Na and Si/Al atomic ratios of 1.22 and 1.15, respectively.

DISCUSSION

Alteration in pure water

The initial dissolution rates measured at 100 °C for Si, B, Na, Al are all 0.8 ± 0.2 g m^{-2} d^{-1}, indicating that the glass dissolves congruently (Fig. 2). This rate is slightly lower than that measured with SON68 glass in the same conditions: 2.0 ± 0.6 g m^{-2} d^{-1} (with the uncertainty of 25% estimated by Fournier et al.[50]) As r_0 is governed by the hydrolysis of Si–O–*M* bonds, the value of r_0 depends on the relative proportion of low-strength bonds

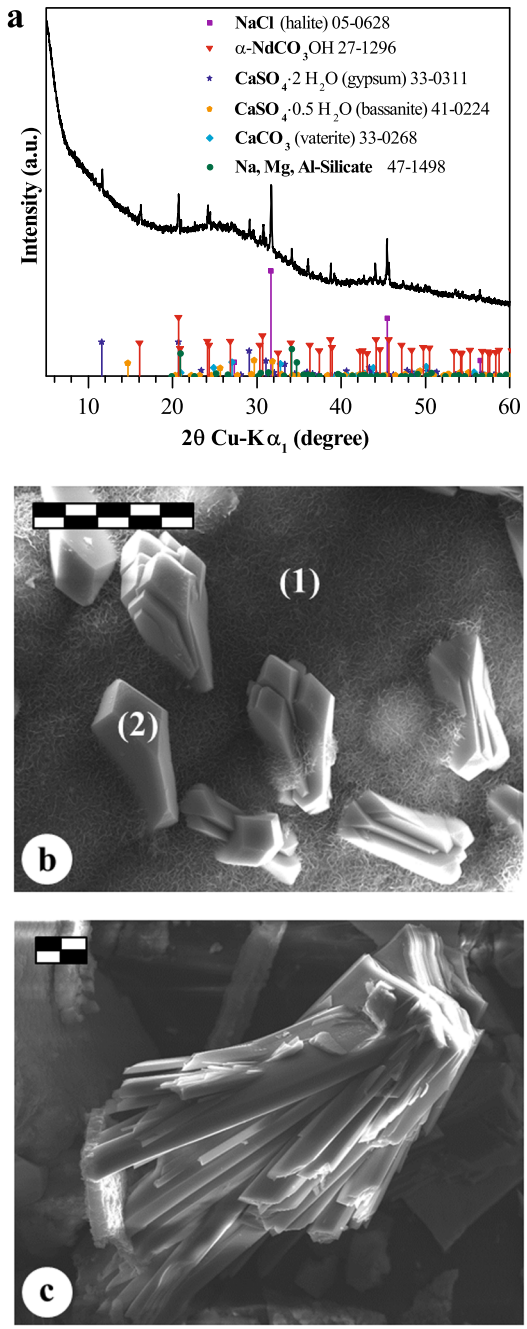

Fig. 5 Post-mortem characterizations of G0.40Nd4C glass after alteration in COx water. **a** X-ray diffractogram showing the precipitation of neodymium hydroxycarbonate (ICDD 27–1296), cristobalite-related sodium magnesiosilicate[63] (ICDD 47–1498), and calcium sulfate and carbonate (ICDD 33–0311, 47–1498, 33–0268). Sodium chloride (ICDD 05–0628) formed on the sample surface as it dried after removing it from the COx water. Backscattered electron scanning micrographs showing the crystallization of **b** phyllosilicates (1), RE carbonate (2), and **c** calcium sulfate. The scale bars represent 10 µm

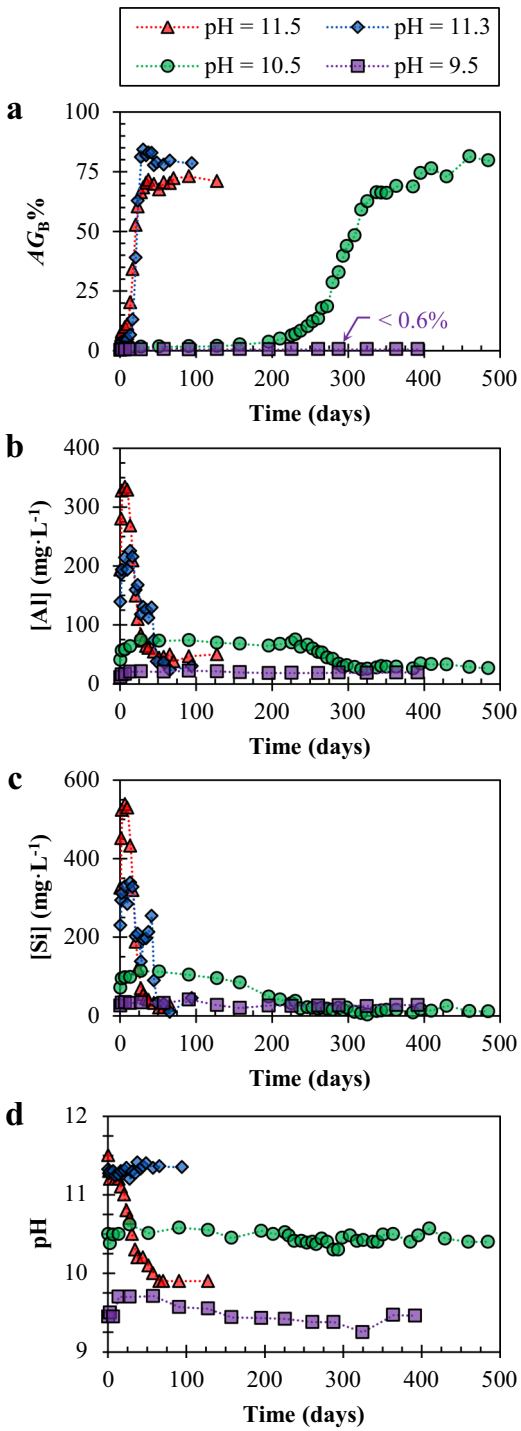

Fig. 6 Alteration in alkaline environments. **a** Time evolution of the altered glass fraction calculated from the amounts of boron released into the solution for G0.40Nd4C glass under static conditions ($T = 90$ °C and $S/V = 40\ cm^{-1}$). **b** Variation of the aluminum concentration. **c** Variation of the silicon concentration. **d** Evolution of the pH measured at 90 °C. At the end of tests at pH = 11.3 and 10.5, the glass is completely altered, although the retention of B (e.g., in calcium borates[64]) explains $AG_B\% < 1$

(e.g., Si–O–B or Si–O^-–Na^+) versus high-strength bonds (e.g., Si–O–Zr or Si–O–Si). According to a previous study[15] the tested peraluminous glass is more polymerized and has a greater amount of high-strength bonds than the SON68 glass (Table 1): this could explain the differences of r_0 observed between these two glasses. The residual rate in the long duration test of the peraluminous glass is roughly 30,000 times lower than the initial rate measured at 100 °C. Given that the thickness of the altered layer remains very low, even after three years of exposure (≈30 nm), its composition and structure could not be characterized.

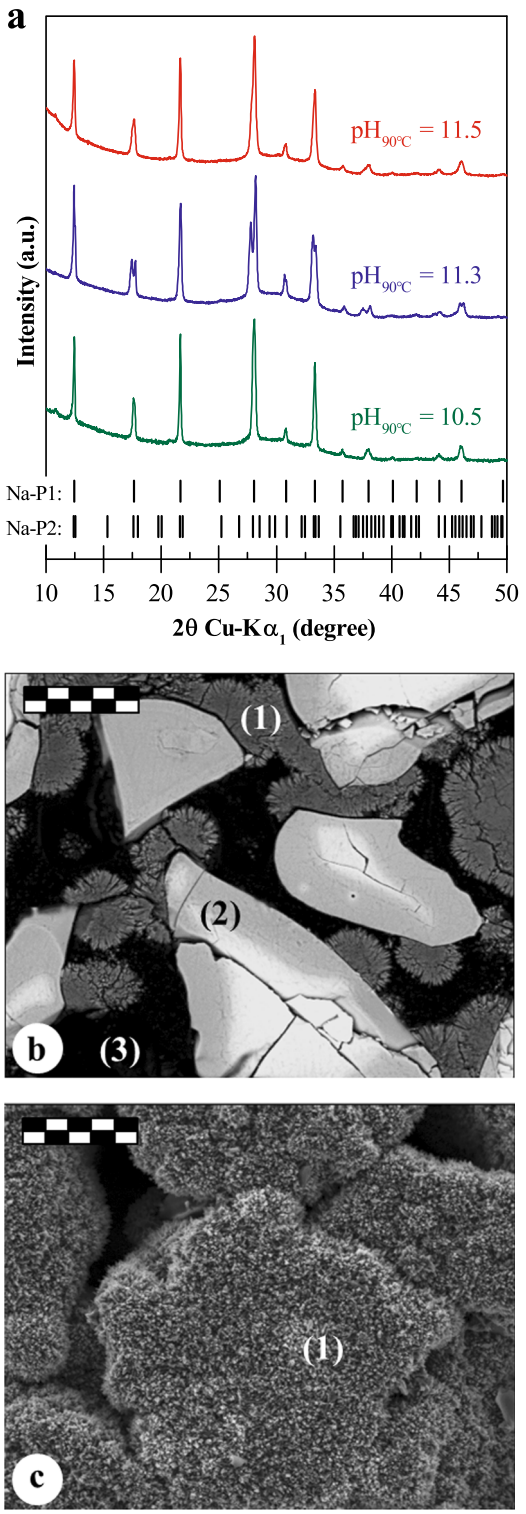

Fig. 7 Post-mortem characterizations of G0.40Nd4C glass after alteration in alkaline environments. **a** X-ray diffractogram showing the precipitation of Na-P1 (ICDD 71–0962) and/or Na-P2 (ICDD 80–0700) zeolites. Scanning electron micrographs after leaching at an initial pH of 11.5 left to vary freely, **b** a cross section (back-scattered electrons) and **c** under secondary electrons observation: (1) zeolites, (2) altered glass, (3) epoxy coating resin. The scale bars represent 50 µm; other enlargements are presented in Supplementary Figure 2

The residual dissolution rate of the peraluminous glass is about one order of magnitude lower than those of the peralkaline ISG and SON68 glasses.[51,52] Its pH and silicon activity under saturation are also lower than these two peralkaline reference glasses. Assuming that the residual rate reflects the passivating effect of the gel depleted in elements that have precipitated as secondary phases,[26,53] these results indicate that the gel which forms on the peraluminous glass is more passivating than those developed on peralkaline glasses or that peraluminous glass is less prone to form secondary phases. Recent studies have shown that the gel that forms under silica saturation and under near-neutral and slightly alkaline pH conditions is the result of in situ reorganization of the silicate network following the removal of the more mobile elements (B, Na, and to a lesser extent Ca).[49,53] This gel formed in these conditions thus partially inherits the structure of its parent glass and does not form large pores. As a consequence, water molecules are highly confined in micropores left by the departure of alkalis and boron. Since the peraluminous glass contains a lower proportion of mobile elements than the peralkaline reference glasses do (Table 1), it may well be that the gel formed under silica saturation conditions is less porous and has less connected pores.

The effect of the chemical environment on the alteration of the peraluminous glass

The composition of aqueous solutions evolves in contact with glass depending on the tendency of the glass and the materials in its vicinity to dissolve and of the newly formed minerals to precipitate, as well as on the diffusive and convective transport properties of water in the evolving confined environment. The aim of studies performed in groundwater and in increasingly alkaline water is to quantify the dominant mechanisms that may promote alteration in a reactive environment.

Alteration in COx water. During the alteration experiment performed with peraluminous G0.40Nd4C glass in COx water, the pH remains below 8 (a lower value than measured for the residual dissolution rate experiment in initially pure water), the concentration of dissolved magnesium decreases, and the average dissolution rate of the glass remains at $3{\cdot}10^{-3}$ g m^{-2} d^{-1} for more than a year, until the Mg concentration in solution drops below 10 mg L^{-1}. Note that there is no magnesium in this glass composition, consequently, the presence of dissolved magnesium in solution is only due to the chemical composition of the COx water.

These properties are the same as those described by Jollivet et al.[40] for the alteration of peralkaline SON68 glass under similar experimental conditions. The proposed mechanism is as follows: the presence of dissolved magnesium leads to the precipitation of magnesium silicates; by taking up the silicon from the solution, this precipitation disrupts the passivating gel and facilitates the dissolution of the glass.

The equation describing the precipitation of a magnesium silicate can be written in terms of the majority species present in solution at pH < 8 (Eq. 1):

$$Mg_xSi_yO_{x+2y-z}(OH)_{2z} = x\,Mg^{2+} + y\,SiO_2(aq) + 2x\,OH^- + (z-x)H_2O \quad (1)$$

The precipitation of magnesium silicate removes a cation, Mg^{2+}, and a non-ionic group, SiO_2(aq), from the solution, and thus also consumes two hydroxide ions (Eq. 1). This buffer effect limits the pH increase. A sufficiently high pH is thus also required for precipitation to occur, alongside sufficient magnesium and silicon concentrations in the solution. The pH threshold above which precipitation can occur depends on the concentrations of magnesium and silicon in the solution and on the composition of the mineral's solubility product.[54,55]

Table 1. Composition of G0.40Nd4C, ISG, and SON68 glasses expressed as molar oxide percentages

Glass	SiO_2	B_2O_3	Na_2O	Al_2O_3	CaO	ZrO_2	Rare-Earth	MgO	Other oxides
G0.40Nd4C	45.5	18.4	5.6	15.0	3.8	2.0	4.1	0.0	5.6
ISG	60.2	16.0	12.6	3.8	5.7	1.7	0.0	0.0	0.0
SON68	52.7	14.0	11.4	3.4	5.0	1.5	1.0	0.0	11.0

The composition of G0.40Nd4C glass is given for a waste content (FPA) of 22.50 mass%

Table 2. Comparison of the alteration of G0.40Nd4C and ISG glasses in sodic solutions at 90 °C

Glass	Si/Al molar ratio in the glass	pH	r_{RA} ($g\,m^{-2}\,d^{-1}$)[a]	Delay before resumption of alteration (d)[b]	[Al] – [Si] concentrations in solution during the plateau time period ($mg\,L^{-1}$)	Si/Al molar ratio in solution	Observed secondary phases
G0.40Nd4C	1.52	11.5[c]	1.0	10–14	334–538	1.54	Na-P1 zeolites
		11.3[d]	1.8	14–17	214–330	1.47	Na-P1 / Na-P2 zeolites
		10.5[d]	0.2	196–211	73–105	1.37	Na-P1 zeolites
		9.5[d]	–	–	19–26	1.32	None
ISG[33,49]	7.92	11.3[d]	1.4	1–2	62–971	15.87	Na-P1 / Na-P2 zeolites, analcime and C-S-H
		11.0[d]	0.9	15–21	50–650	12.05	Na-P1 / Na-P2 zeolites, analcime and C-S-H
		10.7[d]	0.3	29–40	20–277	13.70	Na-P1 zeolites and C-S-H
		10.4[d]	0.02	86–119	11–147	12.84	Na-P1 zeolites

[a]Alteration rates normalized to the specific surface area S_{BET}
[b]Resumption of alteration occurred in between the two indicated time points
[c]pH fixed initially by adding NaOH and then left free to vary
[d]pH maintained throughout the experiment by adding NaOH

Under the *S/V* and temperature conditions considered here, it takes about 300 days for G0.40Nd4C glass to consume 20 mg of dissolved magnesium (Fig. 4), but only about 30 days for the same amount of magnesium to be consumed by SON68 glass.[40] G0.40Nd4C glass thus consumes magnesium more slowly than SON68 glass does. The more limited precipitation of magnesium silicates in the peraluminous domain probably stems from the different compositions of the two glasses. Indeed, the Na_2O content of G0.40Nd4C glass being lower than that of SON68 (4.1 mass% versus 10.1 mass%); the former releases a smaller amount of alkaline species when it dissolves, maintaining a less favorable pH for the precipitation of magnesium silicates.

During the first year of leaching, G0.40Nd4C and SON68 glasses have similar dissolution rates in groundwater (of the order of $10^{-3}\,g\,m^{-2}\,d^{-1}$). Nonetheless, it is important to bear in mind that the magnesium concentration in solution for the experiment with G0.40Nd4C glass is still high after 500 days. The precipitation of magnesium silicates would thus continue beyond 500 days if the pH were to increase. In practice, the rates of magnesium consumption and of glass alteration decrease significantly in between 500 and 900 days. Over longer times (beyond 900 days), it is possible that the magnesium concentration continues to decrease slowly, down to almost zero, if the glass alteration process also continues. Once all the magnesium has been consumed (if not renewed), magnesium silicates cease to form and G0.40Nd4C's dissolution rate will tend toward the value measured in pure water (modified nonetheless by any effects of the pH on the release of mobile species from the glass,[55]) which is roughly one order of magnitude lower than that of SON68 and ISG glasses.

Simply because of its low alkali content, the peraluminous glass is probably less sensitive than previously studied peralkaline glasses to the dissolved magnesium found in underground water and clay minerals.[56,57]

Alteration in pH-controlled solutions. The data from the tests performed in solutions with pHs maintained at between 10.5 and 11.3 and from the experiment performed with a freely varying pH initially set to 11.5 show a sharp increase in the alteration rate after an initial "plateau" time period of variable length (Fig. 6). This phenomenon, which has already been observed for peralkaline glasses, has been dubbed resumption of alteration.[33]

Resumption of alteration rates, r_{RA}, for G0.40Nd4C glass (Table 2) were obtained by linear regression of the data between the first point after the initial plateau and the last point before the final plateau corresponding to the total alteration of the glass (for the tests run at pH 10.5 and 11.3) or to a pH above the zeolite precipitation threshold (for the test performed with pH initially set to 11.5 and then left free to vary). This conventional definition in fact masks complex underlying mechanisms.

In the experiment conducted with an initial pH of 11.5, the pH decreases at the same time as alteration resumes, thus at the same time as the zeolite precipitation begins to consume the alkalinity of the solution. In this test, zeolite precipitation proceeds until the pH drops to 9.9 at which point the altered glass fraction is 73%. Measurement uncertainties and the lack of an alteration tracer make it difficult to know whether this interruption is due to the complete alteration of the glass or to the pH becoming unfavorable for zeolite precipitation. Note in this context that in the experiments conducted with a pH maintained at 10.5 and

11.3, the glass is completely altered and AG_B% reaches 80%. This suggests that a small amount of pristine glass remains in the variable-pH experiment. This would then confirm that the upper pH threshold for zeolite precipitation during the alteration of G0.40Nd4C in a sodic environment is about 9.9, and would also confirm that resumption of alteration self regulates in the absence of an external supply of alkaline species, as it is could be expected.[58]

Comparing the results of the experiments performed at pH 10.5 and 11.3 shows that the higher the pH is, (i) the shorter the plateau time period is and (ii) the higher the rate of resumption of alteration is (multiplied by 9 for a pH difference of 0.8).

The experiments on the peraluminous G0.40Nd4C glass were conducted under conditions similar to those used for the experiments on the peralkaline ISG (same temperature and S_{BET}/V ratio, alkaline solution pHs maintained at similar values) described in Fournier et al.,[59] allowing the two types of glass to be compared. The resumption of alteration of peralkaline glasses is linked with the precipitation of secondary zeolite phases that take up the network forming aluminum and silicon from the glass and the gel.[33,41–43] This study of G0.40Nd4C glass shows that the same mechanisms govern the alteration of peraluminous glasses. The zeolites that form are from the same P family (Fig. 7a) as those identified during the alteration of ISG in alkaline solutions.[44,59] Furthermore, the values of r_{RA} calculated for G0.40Nd4C and ISG (Table 2) are close under similar pH conditions.

However, there are two noteworthy differences between the two glasses: the evolution of the solution concentrations of silicon and aluminum during the resumption, and the delay before resumption of alteration occurs.

The aluminum concentration decreases as zeolites precipitate for both glasses; however, the silicon concentration increases for ISG but decreases for G0.40Nd4C glass. The solubility of the aluminum-depleted gel formed on ISG tends toward that of amorphous silica, whereas the gel formed on G0.40Nd4C glass seems to be less soluble as it contains little silica and a large amount of RE species and Zr.[60]

The delay before resumption of alteration is longer for the peraluminous glass. This can be explained by the composition of the two glasses, which in turn affects the composition of the solution and the nature of the phases that form.

- *The sodium content of the peraluminous glass seems to limit the precipitation of zeolites*. The concentration of Na, which is involved in the formation of sodic zeolites, differs significantly between the two glasses. However, this hypothesis cannot be confirmed in this study because the main source of sodium was the NaOH added to regulate the pH. Nevertheless note that peraluminous glasses release less sodium when dissolving and are therefore less likely to exhibit a resumption of alteration in the absence of an external source of alkalinity. This effect is enhanced by a more substantial release of aluminum into the solution, which lowers the pH.
- *The high aluminum content of the peraluminous glass seems to increase the durability of the passivating gel*. The maximum amount of aluminum consumed by the glass-altering precipitation of zeolites is equal to the amount of aluminum in the gel and in the solution. The amount of altered glass before resumption of alteration is of the same order of magnitude for ISG and G0.40Nd4C glass; however, the amount of aluminum available in the peraluminous system is around four times greater. Assuming that the aluminum consumption rates through zeolite precipitation are identical for the two glasses, the delay before resumption of alteration should be four times greater for the peraluminous one, which is in a good agreement with Table 2 data.
- *The secondary phases that precipitate during the alteration of the peraluminous glass are less detrimental to its durability*. Only P-type zeolites are identified during the alteration of the peraluminous G0.40Nd4C glass whereas for ISG, calcium silicate hydrate (C-S-H) phases are also observed. Furthermore, the P zeolites that precipitate during the alteration of G0.40Nd4C glass are richer in aluminum than those that precipitate in ISG. The precipitation of different phases with different stoichiometries—therefore with different solubilities—modifies the chemistry of the solution and the thermodynamic equilibria. The absence of C-S-H precipitation during the alteration of the peraluminous G0.40Nd4C glass—phases that can act as nucleation sites for zeolites—could be due (i) to a lower silicon concentration in the leaching solutions of G0.40Nd4C than in those of ISG (Supplementary Table 2), and (ii) to the former's lower Ca content.

Concluding remarks

This study of a peraluminous glass with a chemical composition and physico-chemical properties of nuclear interest has shown that the mechanisms governing its alteration are similar to those defined for peralkaline glasses, involving a succession of regimes as alteration proceeds, depending on the leaching conditions: initial rate, rate drop, residual rate, and a possible resumption of alteration. However, the alteration kinetics differ significantly between the peraluminous and peralkaline glasses. Initially, the peraluminous glass investigated here dissolves at a rate of the same order of magnitude as the SON68 peralkaline glass. Thereafter, kinetics data suggest that a passivating gel forms that reduces the dissolution rate of the peraluminous glass by more than four orders of magnitude. This gel seems to be more passivating than the ones formed on ISG and SON68 glasses. Furthermore, the low alkali content and high aluminum content of the peraluminous glass makes it less basic than peralkaline glasses. This means that the likelihood of resumption of alteration through zeolite precipitation is lower than for peralkaline glasses (whose pH in pure water is 9.0–9.3 at 90 °C). Note also that under harsh conditions ($T = 90$ °C and pH > 9.9), the delays before resumption of alteration seem longer for peraluminous glasses than peralkaline ones. Furthermore, a lower pH limits the precipitation of magnesium silicates in COx water. By releasing only small amounts of alkaline species as they dissolve, peraluminous glasses seem less sensitive to their environment and therefore chemically passive, particularly with respect to dissolved magnesium.

MATERIALS AND METHODS

Glass synthesis and sample preparation

The peraluminous glass chosen for this study is referred as G0.40Nd4C. It is a complex glass containing 20 oxides. The 0.40 in the notation represents the $[SiO_2]/[B_2O_3]$ molar ratio and 4 is the molar percentage of Nd_2O_3 (Table 1). The behavior of this glass was compared to that of simplified peralkaline ISG,[46] prepared as described elsewhere,[43] whose composition is given in Table 1.

G0.40Nd4C glass was prepared from oxide powders mixed in a rhodium-plated platinum crucible and heated at 1300 °C for 3 h. The melt was homogenized using a platinum stirrer. A portion of the glass was poured into a graphite crucible and reheated at 630 °C for 30 min and then cooled down to room temperature at 1 °C min^{-1} to allow 2.5 cm × 2.5 cm × 2 mm monoliths to be cut using a diamond saw. These monoliths were polished using an automatic polisher and a series of SiC papers, before a final polishing using a suspension of 1 µm diamond particles. The rest of the glass was poured onto a plate, crushed and sieved to obtain powders with particles 20–40 µm and 63–125 µm in diameter. These powders were cleaned by sedimentation in acetone and absolute grade ethanol to remove the finer particles attached to their surface. Their specific surface area was measured using krypton adsorption measurements and the BET[61] model. The values obtained were respectively 1440 $cm^2\ g^{-1}$ and 480 $cm^2\ g^{-1}$.

Table 3. Conditions used for alteration experiments performed under static conditions for G0.40Nd4C glass

Experiment	PW	GW	pH 9.5	pH 10.5	pH 11.3	pH 11.5
Solution	Pure water	COx water	Alkaline environment, $pH_{90\,°C}$ 9.5	Alkaline environment, $pH_{90\,°C}$ 10.5	Alkaline environment, $pH_{90\,°C}$ 11.3	Alkaline environment, $pH_{90\,°C}$ 11.5
Temperature (°C)	90	90	90	90	90	90
Initial $pH_{90\,°C}$	–	6.01	9.5	10.5	11.3	11.5
pH regulation	No	No	Na(OH)	Na(OH)	Na(OH)	No
Powder particle size (μm)	20–40	63–125	63–125	63–125	63–125	63–125
Powder S_{BET} ($cm^2\ g^{-1}$)	1440	480	480	480	480	480
Glass mass (g)	13.89	0.93	8.25	8.25	8.25	8.25
Solution volume (cm^3)	100	150	100	100	100	100
S/V (cm^{-1})	200	3	40	40	40	40

Table 4. Composition of the synthetic COx water

Element	Na^+	K^+	Mg^{2+}	Ca^{2+}	Sr^{2+}	Si^{4+}	Cl^-	SO_4^{2-}	$pH_{90\,°C}$
Concentration (10^{-3} mol L^{-1})	39.00	0.96	2.50	10.00	0.17	0.84	41.00	10.00	6.0

Experimental parameters

The experimental conditions used for the alteration tests under static conditions are summarized in Table 3.

Alteration in pure water. The initial alteration rate in pure water of G0.40Nd4C glass was determined by alteration of a polished monolith at 100 °C in a Soxhlet apparatus in which the alteration solution was continuously renewed.

The residual alteration rate in initially pure water was determined under static condition at 90 °C in a perfluoroalkoxy (PFA) reactor. The ratio between the glass surface area and the volume of the alteration solution (S/V) was fixed at 200 cm^{-1} (Table 3). A glass monolith was also placed in the solution, in addition to the glass powder. This monolith, which was removed after two months, was used to analyze the altered glass surface by time-of-flight secondary ion mass spectrometry (ToF-SIMS, see the section "Solids analyses").

Alteration in COx water. A sample of G0.40Nd4C glass was altered in laboratory-prepared COx water whose composition is given in Table 4. The pH of the solution was initially adjusted to 6 by CO_2 bubbling. Glass powder was altered under static conditions at 90 °C in a PFA reactor, with an S/V ratio fixed at 3 cm^{-1} (Table 3).

Alteration in alkaline environments. Samples of G0.40Nd4C glass were altered in sodic solutions at pH 11.3, 10.5, and 9.5, at 90 °C, under static conditions, in PFA reactors. These pHs were maintained throughout the tests (±0.15 pH units) by regularly adding NaOH. A sample of G0.40Nd4C glass was also altered in a sodic solution whose pH was initially set to 11.5 and then left free to vary. The S/V ratio for these four tests was 40 cm^{-1} (Table 3).

Analyses of the solutions

At each time point, 2 mL of solution were extracted, passed through a 10 kDa filter, acidified by adding nitric acid, and then analyzed by inductively-coupled plasma optical emission spectroscopy (ICP-OES) to measure the concentrations of Si, B, Al, Na, Ca, and Mg.

Elemental analyses can be used to calculate the percentage of altered glass, $AG_i\%$, for each element, i, (Eq. 2); the equivalent altered glass thickness, eTh_i, or the normalized mass loss, NL_i (Eq. 3); the alteration rate of the glass, r_i (Eq. 4); and the retention factor, f_i, of element i in the gel and in the secondary phases (Eq. 5). Additional details are given in Chave et al.[62]

$$AG_i\%(t) = \frac{c_i(t)\times V(t) + \sum_{j=1}^{t-1} c_i(j)\times V_s(j)}{m\times x_i} \quad (2)$$

In this equation, $c_i(t)$ is the concentration of element i at time t, $V(t)$ is the volume of the solution, $V_s(t)$ is the volume of the jth sample, m is the mass of the glass powder, and x_i is the mass fraction of element i in the glass.

$$eTh_i = \frac{NL_i}{\rho} = \left(1-(1-AG_i\%)^{1/3}\right)\times\frac{3}{\rho\times S_{BET}} \quad (3)$$

In Eq. 3, ρ is the density of the glass, S_{BET} its specific surface area, and $3/(\rho\times S_{BET})$ the mean initial radius of a glass particle. In practice, a glass alteration rate is calculated by the sliding average over three successive points.

$$r_i = \frac{d}{dt}NL_i \quad (4)$$

Retention factors are calculated according to Eq. 5, where NL_T is the normalized mass loss calculated with respect to the alteration tracer, i.e., an element that is not retained either in the gel or in the secondary phases.

$$f_i = 1 - \frac{NL_i}{NL_T} \quad (5)$$

Solids analyses

Diffractograms were recorded using a Phillips X'PERT Pro PANalytical device equipped with a monochromatic Cu-Kα ($\lambda = 1.5418$ Å) source operating at 40 mA and 40 kV in Bragg-Brentano geometry. The sample was first crushed into a fine powder to randomize the orientation of the crystals. The data were acquired over a 4–80° 2θ range at 0.11°·min^{-1} in 0.017° steps.

The samples were observed using a Philips XL30 scanning electron microscope equipped with a tungsten filament (acceleration voltage, 15 kV) and attached to an energy dispersive X-ray (EDX) detector. The samples were first coated in epoxy resin, polished with a series of SiC papers and then a suspension of 1 μm diamond particles, and finally metalized.

Elemental profiles in the altered layer of glass monolith altered in presence of pure water were measured by ToF-SIMS (IONTOF TOF 5). The profiles were obtained by alternating abrasion and analysis. Abrasion was carried out with a 500 eV, 47 nA primary O_2^+ ion beam on an area measuring 250 μm × 250 μm; analysis was performed with a 25 keV Bi_1^+ ion beam at 2 pA on an area measuring 50 μm × 50 μm. Surface charges on the monoliths were neutralized using a pulsed low-energy (<20 eV) electron flux. The depths of the elemental profiles were calibrated using a

profilometer measurement of the crater depth. All the elemental intensities were normalized with respect to the signal from the Bi_1^+ ion to avoid possible matrix effects. To mitigate the effect of primary current variations, the intensity of each isotope was normalized with respect to the main isotope of the glass, i.e., ^{28}Si. The elemental profile $C(i)/C_g$ of an element i was normalized to that of Zr (because Zr remains immobile during glass corrosion in the experimental conditions concerned[60]) and the ratio i/Zr was then normalized with respect to that measured in the pristine glass as shown in Eq. 6.

$$\frac{C(i)}{C_g} = \frac{(i/\mathrm{Zr})_{\text{altered glass}}}{(i/\mathrm{Zr})_{\text{pristine glass}}} \quad (6)$$

A ratio $C(i)/C_g < 1$ in the altered glass means that the altered glass was depleted in element i compared with the pristine glass, whereas a ratio $C(i)/C_g > 1$ indicates that the altered glass was enriched in element i. The transition between the altered glass and the pristine glass was defined as corresponding to a $C(i)/C_g$ ratio of 0.5.

Data availability statement

The authors declare that the data supporting the findings of this study are available within the article and its supplementary information files.

ACKNOWLEDGEMENTS

The authors wish to thank Estelle Gasnier for passing on the understanding of peraluminous glasses (their formulation, network structure, and crystallization behavior) she acquired between 2010 and 2013. Financial support from the CEA (French alternative energies and atomic energy commission, Marcoule, France), from AREVA (France) and from EDF (Electricité de France, France) is gratefully acknowledged.

AUTHOR CONTRIBUTIONS

V.P. performed the experiments and wrote the paper. I.B.-G., V.M., and N.P. supervised the materials studies (formulation, preparation, and characterization of the glasses). P. J., P.F., M.F., and S.G. supervised the leaching experiments and the interpretation of the data. I.B.-G., M.F., P.J., P.F., and S.G. were deeply involved in reviewing the paper.

ADDITIONAL INFORMATION

Supplementary information accompanies the paper on the *npj Materials Degradation* website (https://doi.org/10.1038/s41529-018-0028-3).

Competing interests: The authors declare no competing financial interests.

Publisher's note: Springer Nature remains neutral with regard to jurisdictional claims in published maps and institutional affiliations.

REFERENCES

1. Gin, S., Jollivet, P., Tribet, M., Peuget, S. & Schuller, S. Radionuclides containment in nuclear glasses: an overview. *Radiochim. Acta* **105**, 927–959 (2017).
2. Pacaud, F., Jacquet-Francillon, N., Terki, A. & Fillet, C. R7T7 light water reference glass sensitivity to variations in chemical composition and operating parameters. *Mater. Res. Soc. Symp. Proc.* **127**, 105–112 (1988).
3. Frugier, P., Martin, C., Ribet, I., Advocat, T. & Gin, S. The effect of composition on the leaching of three nuclear waste glasses: R7T7, AVM and VRZ. *J. Nucl. Mater.* **346**, 194–207 (2005).
4. Gras, J.-M. et al. Perspectives on the closed fuel cycle – implications for high-level waste matrices. *J. Nucl. Mater.* **362**, 383–394 (2007).
5. Lopez, C. et al. Solubility of actinide surrogates in nuclear glasses. *J. Nucl. Mater.* **312**, 76–80 (2003).
6. Kidari, A. et al. Lanthanum and neodymium solubility in simplified SiO_2– B_2O_3–Na_2O – Al_2O_3–CaO high level waste glass. *J. Am. Ceram. Soc.* **95**, 2537–2544 (2012).
7. Kidari, A. et al. Solubility and partitioning of minor-actinides and lanthanides in alumino-borosilicate nuclear glass. *Procedia Chem.* **7**, 554–558 (2012).
8. Li, H., Li, L., Strachan, D. M. & Qian, M. Optical spectroscopy study of neodymium in sodium alumino-borosilicate glasses. *J. Non-Cryst. Solids* **349**, 127–132 (2004).
9. Li, L., Li, H., Qian, M. & Strachan, D. M. Gadolinium solubility in peraluminous borosilicate glasses. *J. Non-Cryst. Solids* **281**, 189–197 (2001).
10. Li, L., Li, H., Qian, M. & Strachan, D. M. Gadolinium solubility in peralkaline borosilicate glasses. *J. Non-Cryst. Solids* **283**, 237–245 (2001).
11. Li, L., Strachan, D. M., Li, H., Davis, L. L. & Qian, M. Crystallization of gadolinium- and lanthanum-containing phases from sodium alumino-borosilicate glasses. *J. Non-Cryst. Solids* **272**, 46–56 (2000).
12. Qian, M., Li, L., Li, H. & Strachan, D. M. Partitioning of gadolinium and its induced phase separation in sodium-aluminoborosilicate glasses. *J. Non-Cryst. Solids* **333**, 1–15 (2004).
13. Caurant, D., Loiseau, P. & Bardez, I. Structural characterization of Nd-doped Hf-zirconolite $Ca_{1-x}Nd_xHfTi_{2-x}Al_xO_7$ ceramics. *J. Nucl. Mater.* **407**, 88–99 (2010).
14. Caurant, D. et al. Crystallization of neodymium-rich phases in silicate glasses developed for nuclear waste immobilization. *J. Nucl. Mater.* **354**, 143–162 (2006).
15. Gasnier, E. et al. Homogeneity of peraluminous SiO_2–B_2O_3–Al_2O_3–Na_2O–CaO–Nd_2O_3 glasses: effect of neodymium content. *J. Non-Cryst. Solids* **405**, 55–62 (2014).
16. Piovesan, V., Bardez-Giboire, I., Perret, D., Montouillout, V. & Pellerin, N. Effect of composition on peraluminous glass properties: an application to HLW containment. *J. Nucl. Mater.* **483**, 90–101 (2017).
17. Vienna, J. D., Ryan, J. V., Gin, S. & Inagaki, Y. Current understanding and remaining challenges in modeling long-term degradation of borosilicate nuclear waste glasses. *Int. J. Appl. Glass Sci.* **4**, 283–294 (2013).
18. Jantzen, C. M., Brown, K. G. & Pickett, J. B. Durable glass for thousands of years. *Int. J. Appl. Glass Sci.* **1**, 38–62 (2010).
19. Grambow, B. Nuclear waste glasses; how durable? *Elements* **2**, 357–364 (2006).
20. Gin, S. Open scientific questions about nuclear glass corrosion. *Procedia Mater. Sci.* **7**, 163–171 (2014).
21. Boksay, Z., Bouquet, G. & Dobos, S. Kinetics of formation of leached layers on glass surfaces. *Phys. Chem. Glass* **9**, 69–71 (1968).
22. Doremus, R. H. Interdiffusion of hydrogen and alkali ions in a glass surface. *J. Non-Cryst. Solids* **19**, 137–144 (1975).
23. Bunker, B. C. Molecular mechanisms for corrosion of silica and silicate glasses. *J. Non-Cryst. Solids* **179**, 300–308 (1994).
24. McGrail, B. P. et al. The structure of Na_2O–Al_2O_3–SiO_2 glass: impact on sodium ion exchange in H_2O and D_2O. *J. Non-Cryst. Solids* **296**, 10–26 (2001).
25. Ojovan, M. I., Pankov, A. & Lee, W. E. The ion exchange phase in corrosion of nuclear waste glasses. *J. Nucl. Mater.* **358**, 57–68 (2006).
26. Frugier, P. et al. SON68 nuclear glass dissolution kinetics: current state of knowledge and basis of the new GRAAL model. *J. Nucl. Mater.* **380**, 8–21 (2008).
27. Casey, W. H. & Bunker, B. C. Leaching of mineral and glass surfaces during dissolution. *Rev. Mineral. Geochem.* **23**, 397–426 (1990).
28. Jollivet, P., Gin, S. & Schumacher, S. Forward dissolution rate of silicate glasses of nuclear interest in clay-equilibrated groundwater. *Chem. Geol.* **330-331**, 207–217 (2012).
29. Grambow, B. A general rate equation for nuclear waste glass corrosion. *Mater. Res. Soc. Symp. Proc.* **44**, 15–27 (1984).
30. Bourcier, W. L., Peiffer, D. W., Knauss, K. G., McKeegan, K. D. & Smith, D. K. A kinetic model for borosilicate glass dissolution affinity of a surface alteration layer. *Mater. Res. Soc. Symp. Proc.* **176**, 209–216 (1989).
31. Grambow, B. & Müller, R. First-order dissolution rate law and the role of surface layers in glass performance assessment. *J. Nucl. Mater.* **298**, 112–124 (2001).
32. Gin, S. et al. Nuclear glass durability: new insight into alteration layer properties. *J. Phys. Chem. C.* **115**, 18696–18706 (2011).
33. Fournier, M., Gin, S. & Frugier, P. Resumption of nuclear glass alteration: state of the art. *J. Nucl. Mater.* **448**, 348–363 (2014).
34. Neill, L. et al. Various effects of magnetite on international simple glass (ISG) dissolution: implications for the long-term durability of nuclear glasses. *npj Mater. Degrad* **1**, 1 (2017).
35. Burger, E. et al. Impact of iron on nuclear glass alteration in geological repository conditions: a multiscale approach. *Appl. Geochem.* **31**, 159–170 (2013).
36. McVay, G. L. & Buckwalter, C. Q. Effect of iron on waste-glass leaching. *J. Am. Ceram. Soc.* **66**, 170–174 (1983).
37. Michelin, A. et al. Silicate glass alteration enhanced by iron: origin and long-term implications. *Environ. Sci. Technol.* **47**, 750–756 (2013).
38. Michelin, A. et al. Archeological slag from Glinet: an example of silicate glass altered in an anoxic iron-rich environment. *Chem. Geol.* **413**, 28–43 (2015).
39. Dillmann, P., Gin, S., Neff, D., Gentaz, L. & Rebiscoul, D. Effect of natural and synthetic iron corrosion products on silicate glass alteration processes. *Geochim. Cosmochim. Acta* **172**, 287–305 (2016).
40. Jollivet, P. et al. Effect of clayey groundwater on the dissolution rate of the simulated nuclear waste glass SON68. *J. Nucl. Mater.* **420**, 508–518 (2012).
41. Gin, S. & Mestre, J. P. SON 68 nuclear glass alteration kinetics between pH 7 and pH 11.5. *J. Nucl. Mater.* **295**, 83–96 (2001).
42. Ribet, S. & Gin, S. Role of neoformed phases on the mechanisms controlling the resumption of SON68 glass alteration in alkaline media. *J. Nucl. Mater.* **324**, 152–164 (2004).

43. Gin, S. et al. The fate of silicon during glass corrosion under alkaline conditions: a mechanistic and kinetic study with the International Simple Glass. *Geochim. Cosmochim. Acta* **151**, 68–85 (2015).
44. Fournier, M., Frugier, P. & Gin, S. Resumption of alteration at high temperature and pH: rates measurements and comparison with initial rates. *Procedia Mater. Sci.* **7**, 202–208 (2014).
45. Ebert, W. L. & Bates, J. K.A comparison of glass reaction at high and low glass surface/solution volume. *Nucl. Technol.* **104**, 372–384 (1993).
46. Gin, S. et al. An international initiative on long-term behavior of high-level nuclear waste glass. *Mater. Today* **16**, 243–248 (2013).
47. Collin, M. et al. Structure of international simple glass and the properties of passivating layer formed in circumneutral pH conditions. *npj Mater. Degrad.* in press (2017).
48. Molières, E. et al.Chemical durability of lanthanum-enriched borosilicate glass. *Int. J. Appl. Glass Sci.* **4**, 383–394 (2013).
49. Gin, S. et al. Atom-probe tomography, TEM and ToF-SIMS study of borosilicate glass alteration rim: a multiscale approach to investigating rate-limiting mechanisms. *Geochim. Cosmochim. Acta* **202**, 57–76 (2017).
50. Fournier, M. et al. Glass dissolution rate measurement and calculation revisited. *J. Nucl. Mater.* **476**, 140–154 (2016).
51. Gin, S., Frugier, P., Jollivet, P., Bruguier, F. & Curti, E. New insight into the residual rate of borosilicate glasses: effect of S/V and glass composition. *Int. J. Appl. Glass Sci.* **4**, 371–382 (2013).
52. Gin, S., Beaudoux, X., Angéli, F., Jégou, C. & Godon, N. Effect of composition on the short-term and long-term dissolution rates of ten borosilicate glasses of increasing complexity from 3 to 30 oxides. *J. Non-Cryst. Solids* **358**, 2559–2570 (2012).
53. Gin, S. et al. Origin and consequences of silicate glass passivation by surface layers. *Nat. Commun.* **6**, 6360 (2015).
54. Aréna, H. et al. Impact of iron and magnesium on glass alteration: characterization of the secondary phases and determination of their solubility constants. *Appl. Geochem.* **82**, 119–133 (2017).
55. Chave, T., Frugier, P., Ayral, A. & Gin, S. Solid state diffusion during nuclear glass residual alteration in solution. *J. Nucl. Mater.* **362**, 466–473 (2007).
56. Debure, M., Frugier, P., De Windt, L. & Gin, S. Borosilicate glass alteration driven by magnesium carbonates. *J. Nucl. Mater.* **420**, 347–361 (2012).
57. Debure, M., De Windt, L., Frugier, P. & Gin, S. HLW glass dissolution in the presence of magnesium carbonate: diffusion cell experiment and coupled modeling of diffusion and geochemical interactions. *J. Nucl. Mater.* **443**, 507–521 (2013).
58. Fournier, M. *Etude des mécanismes à l'origine des reprises d'altération. Modélisation et évaluation de l'impact sur les verres de confinement (Study of the mecanisms underlying resumptions of alteration. Modeling and evaluation of the impact on nuclear waste glasses)*, Ph.D. Thesis, (University of Montpellier, Montpellier, 2015).
59. Fournier, M., Gin, S., Frugier, P. & Mercado-Depierre, S. Contribution of zeolite seeded experiments to the understanding of resumption of glass alteration. *npj Mater. Degrad.* **1**, 17 (2017).
60. Cailleteau, C. et al. Insight into silicate-glass corrosion mechanisms. *Nat. Mater.* **7**, 978–983 (2008).
61. Brunauer, S., Emmett, P. H. & Teller, E. Adsorption of gases in multimolecular layers. *J. Am. Chem. Soc.* **60**, 309–319 (1938).
62. Chave, T., Frugier, P., Gin, S. & Ayral, A. Glass-water interphase reactivity with calcium rich solutions. *Geochim. Cosmochim. Acta* **75**, 4125–4139 (2011).
63. Withers, R. L., Lobo, C., Thompson, J. G., Schmid, S. & Stranger, R. A modulation wave approach to the structural characterization of three new cristobalite-related sodium magnesiosilicates. *Acta Cryst. B* **53**, 203–220 (1997).
64. Mercado-Depierre, S., Angeli, F., Frizon, F. & Gin, S. Antagonist effects of calcium on borosilicate glass alteration. *J. Nucl. Mater.* **441**, 402–410 (2013).